Outcrop distribution and formation of carbonate rhizoliths in Badain Jaran Desert, NW China

Qingfeng Sun, Arnaud Huguet, Kazem Zamanian

Outcrop distribution and formation of carbonate rhizoliths in Badain Jaran Desert, NW China

Qingfeng Sun[a,*], Arnaud Huguet[b], Kazem Zamanian[c]

[a] *Faculty of Geography, Northwest Normal University, Lanzhou 730070,China*

[b] *Sorbonne Université, CNRS, EPHE, PSL, UMR METIS, F-75005 Paris, France*

[c] *Department of Soil Science of Temperate Ecosystems, Georg-August University of Goettingen, Buesgenweg 2, 37077 Goettingen, Germany*

**Corresponding author. Email address: sqf@nwnu.edu.cn*

Abstract

Carbonate rhizoliths and related features are environmental and ecological indicators of not only palaeosols, but also modern soils. They designate subaerial vadose and pedogenic diagenesis environments. Rhizoliths are commonly used as a tool for paleoenvironmental reconstructions, but uncertainty remains regarding their formation mechanisms. Field characteristics of the dune rhizoliths in the Badain Jaran Desert, NW China were analyzed to investigate formation mechanisms and interpret paleoenvironmental significance. Systematic field sampling and intensive examination showed that the tube-like rhizoliths without morphological structures of plant roots have been placed at the dune soil surface following erosion and weathering but the underground rhizoliths are still connected to the dead *Artemisia* roots. Rhizoliths occurred only along the windward, long gentle slopes of mega-dunes. Their distribution patterns of both types in connection with plant distribution and landscapes have been studied. Their petrological and mineralogical characters were performed in detail using microscopic and spectroscopic techniques (cathodoluminescence, scanning electronic microscopy and energy dispersive X-ray spectroscopy) in laboratory. Altogether, field and laboratory analyses showed that rhizolith cement is calcium carbonate and despite the high porosity of soil and high aridness of climate,

soil moisture plays an important role in sustaining *Artemisia* growth and rhizolith formation. Desert rhizoliths can therefore be used as a proxy to infer local soil moisture and plant communities. Moreover, as soil moisture content is related to climate and landscape position, rhizoliths could indirectly be indicators of aboveground environmental conditions, e.g. annual precipitation or humidity.

Keywords

Rhizoliths; Dune soil; Deflation and weathering; Formation factors; Soil environment

1. Introduction

Rhizolith, an umbrella term, has been used widely and includes many sub-terms, such as root tubules, root casts, root moulds, rhizocretions, root petrifactions, rhizolites, rhizomorphs, hypocoatings, rhizohalo, calcified root cells, and *Microcodium* (e.g. Klappa, 1980; Košir, 2004; Kraus and Hasiotis, 2006; Barta, 2011). All these sub-terms are somewhat defined by the morphological features associated with their strata, sediments, or soils where they were persevered. Hence, morphological features of rhizoliths provide important evidence for rhizolith research. The cementing minerals of rhizoliths can be carbonate, silica, clay, jarosite and rhodochrosite-siderite (e.g., Kraus and Hasiotis, 2006; Owen et al., 2008; Bojanowski et al., 2016). Carbonate is the most common one among them (e.g. Sun et al., 2019a). Carbonate rhizoliths occur frequently in Quaternary terrestrial aeolianites of coastal regions (e.g., Klappa, 1980), dunes (e.g., Cramer and Hawkins, 2009; Golubtsov et al., 2019), loess-palaeosol sequences (e.g. Wang et al., 2004; Gocke et al., 2010, 2011, 2014; Barta, 2011; Huguet et al., 2012, 2013.), eolian rocks and eolian sand bodies (e.g. Loope, 1988), as well as lake margins (e.g., Owen et al., 2008; Sun et al., 2019a).

The texture and composition of Quaternary calcareous dune soils and the climatic settings in desert especially provide optimal conditions for the development of rhizoliths (e.g., Loope, 1988; Golubtsov et al., 2019), which are abundant and of large size in such environments (e.g., Klappa, 1980; Rao and Thamban, 1997; Alonso-Zarza et al., 2008; Roberts et al., 2008; Cramer and Hawkins, 2009).

Rhizolith architecture and geometry is highly dependent on root type as well as diagenetic and pedogenic parameters. Even though most rhizoliths do not retain the morphological structures of their source plants (Sarjeant, 1975), they can still be used to make some qualitative and quantitative inferences about the densities, sizes and types of former vegetation ecosystem (Pfefferkorn and Fuchs, 1991; Rinehart et al., 2015). Moreover, rhizoliths and the related features are also indicators of paleosols and hence of subaerial vadose environments in ancient successions and are widely used as a tool for paleoenvironmental reconstructions (e.g., Klappa, 1980; Golubtsov et al., 2019; Nascimento et al, 2019; Sun et al., 2019a). Yet, the paleoecological and paleoenvironmental studies based on rhizoliths often came across difficulties in interpretation of ^{14}C ages and the stable isotope composition of carbonate cement (Sun et al., 2019). This is mostly due to the inclusion of lithogenic carbonates from the enclosing deposits and recrystallization of deposited carbonates as rhizolith cement (e.g. Gocke et al., 2011; Sun et al., 2019b; Golubtsov et al., 2019). Furthermore, the formation mechanisms of rhizoliths in sedimentary environment, especially deserts, still remain highly uncertain (Sun et al., 2019a).

Carbonate rhizoliths (Sun et al., 2019b) or carbonate root tubes (Li et al., 2017) have been previously investigated in the dunes of the deserts of the Alashan Plateau, especially in the Badain Jaran Desert, Northwest China, (Gao et al., 1993; Yang, 2000; Yang et al., 2003; Chen et al., 2004; Li et al., 2015a, b; Li et al., 2017; Zhu et al., 2019;

77 Sun et al., 2019b). However, it is still unclear whether the rhizolith records can be
78 effectively used to reconstruct the paleovegetation. Much remains unknown about the
79 impact of fossilization processes, even though these may introduce biases into
80 palaeobiological interpretations. Systemic studies of rhizolith features are still scarce
81 and rudimentary in this area (Li et al., 2017; Sun et al., 2019b), despite usually large
82 numbers of rhizoliths can be found, especially, on a vast area, which provides good
83 data for rhizoliths study. Most importantly and firstly, rhizoliths study relies on the
84 field description of fossil morphologies to understand the evolutionary history of plant
85 and the fossilization mechanism. Fossil morphologies under field conditions remain
86 poorly understood. Therefore, this project focuses on the intensive analyzing
87 topographical distributions and architectural patterns of rhizoliths in the field. We
88 further examined the macro- and micromorphological characteristics of the cementing
89 minerals of the collected rhizoliths from the desert in laboratory. Altogether, these
90 characterizations aim to achieve a better understanding of rhizoliths formation
91 mechanisms and help in ascertaining the paleoenvironmental interpretations (Li et al.,
92 2015a, b; Li et al., 2017 ; Zhu et al., 2019) and ^{14}C dating previously made by using
93 these objects (Sun et al., 2019b) .
94

95 2. Geographical setting of Badain Jaran Desert

96 The Badain Jaran Desert (39°04′15″N to 42°12′23″N, 99°23′18″E to 104°34′02″E)
97 is located in northwestern China (Fig. 1). This desert comprises the tallest mega-dunes
98 in the world, with interdunal lakes frequently occurring between the dunes. The
99 mega-dunes are especially dense and high in the southeastern part, where they can
100 reach up to 500 m a.s.l (Wang et al., 2005; Zhu et al., 2010; Yang et al., 2011; Wang et
101 al., 2015).

This desert is an arid desert climate according to the Köppen climate classification (Kottek et al., 2006). The annual precipitation is currently 40–120 mm, falling mainly in summer, and the annual potential evaporation is over 2500 mm. The conventional precipitation (below 5 mm) accounts for approximately 90% of rainfall events (Wang et al., 2013). The mean annual air temperature ranges between 9.8 and 10.2°C. The prevailing cold-arid winter wind direction is northwest and the strongest winds occur in spring and the mean annual wind speed ranges between 2.8 and 4.6 m/s (Fig. 1, Dong et al., 2004; Hu et al., 2015; Zhang et al., 2017).

The vegetation of this desert is dominated by shrubs and subshrubs, including *Haloxylon, Nitraria, Tamarix,* and *Reaumuria* species (Wang et al., 2015a). Perennial woody *Artemisia scoparia* and herbaceous *Psammochloa villosa* and *Phragmites australis* grow on the mega-dunes due to the existence of moist sand layers.

The grain size of surface sand layers is dominated by well-sorted, rounded, pinky-grey, middle to fine sand, containing only a slight amount of melanocratic minerals (such as hornblende, pyroxene and magnetite), with carbonates minerals being less abundant in the silicate desert sands (Gates et al., 2008; Bai, 2011). The average carbonate content in soils was reported as 4.6 % by Wang et al. (2004) and 6.5 % by Sun et al. (2019b). The thickness of the upper dry soil of the mega-dune is only about 20 cm, with a conspicuous moist soil under it. The water content (by weight) is usually 1-5% between 0.2-1.5 m depths (Gu et al., 2004; Zhao et al., 2011; Wang et al., 2019) and is up to 10% at 90 cm depth with well-preserved sand bedding (Liu et al., 2016). At 2.0-8.3 m depth, water contents vary between 2-5.0% (Zhao et al., 2011). The high moisture is in low-lying and flat land, which is benefited from the precipitation infiltration (Zhao et al., 2011).

Mega-dunes feature that small transverse dunes superimposed on the larger

transverse dunes can be classified into three hierarchical orders (Fig. 2, Dong et al., 2009). Order III corresponds to an erosion belt, next to the shore of lakes; Order II is a belt of both erosion and deposition above Order III; and Order I is a deposition belt. Order III and II are situated on the windward gentle slopes and Order I dunes correspond to the leeward slopes (slipface), which are steep and even.

3. Field survey, examination and sampling

Owing to the vast sand sea area, poor accessibility and the dominance of an extremely arid climate, field explorations are only conducted in zones located in the southeastern part next to the desert margin (Fig. 1). Along the exploration route of about 400 km in the hinterland of the desert, rhizoliths were only found at four sites (Fig. 1, red points A-D), which form a profile from the central part to the margin of the desert (Sites A-B-C-D, Fig. 1). Detailed survey and examinations of landscape, vegetation, modern root, sediment/soil, rhizolith exposure and morphology were carried out around the four sites. At each site the most representative samples of carbonate rhizoliths and their typical features were intensively described and photographed. Typical rhizoliths were delicately handled for field photographing and transported to the laboratory.

4. Laboratory analyses

Eight rhizolith samples (two from each site) were analyzed in the laboratory. The applied analytical methods were microscopy, cathodoluminescence, staining, scanning electronic microscopy - energy dispersive X-ray spectroscopy, which are all performed at the Institute of Northwest Petroleum Geology, Lanzhou, China. Zeiss Scope A1 microscope was used to examine mineral crystal morphology. A staining method (a mixture of Alizarin red S and potassium ferricyanide) was used to analyze

the carbonate minerals in the cement under the microscope (Dickson 1965, 1966); CITL CL8200 MK5 cathodoluminescence (CL) instrument was used to investigate the luminescence color of cement. The micro-scale morphology and chemical compositions of the rhizolith cement were determined by scanning electron microscopy (SEM; FEI Quanta 450) coupled with Energy dispersive X-ray spectroscopy (EDS). Each rhizolith specimen was first impregnated with and without resin cover respectively, cut and polished to 4.8 cm×2.8 cm slices made from transverse sections, and then described by polarizing microscopy and cathodoluminescence. Fragments of the rhizoliths were gold coated, and then analyzed by SEM coupled with EDS.

5. Results

5.1. Field features of rhizoliths

5.1.1 Geomorphological distributions of rhizolith outcrops

In Site A (Sumujilin Lake, 39°48’N, 102°26’E), the rhizolith outcrops were found at the foot of the windward gentle slope of the mega-dune, located east of the Sumujilin Lake (Fig. 3a). This site is on the eroded area of Order III, which is flatter than the upper zone along the windward slope (Figs. 2a; 3a).

In Site B (Nuoertu Lake, 39°46’N, 102°27’E), rhizolith outcrops were found along the upper gentle slope (Order II) of the mega-dune on the east side of the Nuoertu Lake (Fig. 4a).

In Site C (Baoritaolegai Lakes, 39°35’N, 102°28’E), rhizoliths occur along the whole windward gentle slope (Order III,II) of a mega-dune, south of Baoritaolegai Lake(Fig. 5a).

Site D (39°27’N, 102°26’E) is near to (6 km to the east) the Gate of the Badain

Jaran Desert National Geological Park, which is located at the southern-eastern margin of the desert, where small low dunes dominate (Figs. 1; 6a). Rhizolith outcrops occur within the swales between the dunes. In addition to *Psammochloa*, *Artemisia* is the dominant vegetation in the area, usually growing in the gentle windward slopes of the swales (Fig.6a).

5.1.2 Field characteristics of rhizolith specimen

In Site A, rhizolith fragments are eroded out of the sand, together with caliche fragments (sand soil cemented by carbonates) (Fig. 3b). This slope of the mega-dune covered by fragments of the rhizolith and caliche is purple-brown, obviously different from the beige color of the above dune sand along the whole slope (Fig. 3a). The fragments of typical rhizoliths are hard and varnished brightly. Their centers are tubular cavities (Fig. 3c). Except sparse *Psammochloa villosa,* no other vegetation grows in the area of the rhizolith outcrops.

In Site B, at low altitude, rhizoliths occurred mostly as enormous coarse brown fragments, similar to Site A. At high altitude, the rhizolith tubes are long and white, branchy or separated (Fig. 4b) in some places. Relicts of fine root hairs were observed. (Fig. 4c).

In Site C, besides usual fragments of straight short tubes, thin tubes with many lateral fine root hairs and thick tubes with hemp rope-like striations were found (Fig. 5b). Primary rhizoliths were found under semi-arid/moist sandy soil (depth ~ 10 cm) at locations where *Artemisia* was rooted. They are softer and thicker than those eroded out of soil (Fig. 5c). The eroded-out tubes were constituted of either double cemented layers or often a singular layer (Fig. 5d). In addition, the walls of the rhizoliths containing plant relicts were thicker than those without root relicts (Fig. 5e).

In Site D (39^{o}27’N, 102^{o}26’E), rhizolith fragments are present on the sand

surface (Fig. 6b) and a few of them are in situ vertically within the sand (Fig. 6b). The vertical rhizoliths below ground correspond to pristine rhizoliths, without any signs of erosion and insolation, and are much thicker than those found aboveground (Fig. 6c). Once broken, the root remains within the tubes of the pristine rhizoliths appear as surrounded by white haloes of cement (Fig. 6d).

5.2. Laboratory results

Two rhizoliths from each site were chosen randomly for laboratory analyses. Staining and cathodoluminescence analyses confirmed that the cementing minerals of the rhizoliths are carbonate, and the clastic particles are quartz and feldspars (Fig. 7a, b). Cathodoluminescence observations indicated that calcium ions for carbonate cement should come from the chemical weathering of feldspars (Fig. 7b). SEM and EDS analyses showed that the carbonate cement was mainly calcite and low-magnesium calcite, with only a slight amount of NaCl (Figs. 7c, d). The bulk characteristics of the rhizoliths from the four sites were generally similar, with carbonate minerals being the cement of hard rhizoliths formed in the dune sands.

6. Discussion

6.1. Classification and environmental implications of rhizoliths

The rhizoliths from the four investigated sites were classified as tubules, or tubes (Li et al., 2015a, b) based on their field features. Only a few of dead root remains were found in the tubes, which indicate no root petrification or body fossilization took place through diagenesis. The central voids were occasionally filled with loose aeolian sand after weathering. Hypocoating occurred through pedogenesis forming secondary carbonates as hard tube walls, as confirmed by SEM-EDS analyses (calcite

and low-Mg calcite being predominant; Fig. 7d).

According to the rhizoliths formation locations, two types of rhizoliths, present in different zones of the soil, were observed: (i) primary ones and (ii) eroded-out-weathered ones. Primary rhizoliths are in situ in the soil, which allowed the preservation of their primary state - vertical but also rarely horizontal, soft and thick (Figs. 5c; 6b, c, d). In contrast, the eroded-out-weathered rhizoliths were apparent out of the soil, weathered and eroded at the surface, being hard and thin. This indicates that strong wind deflation eroded the surface soil around the sampling site, likely removing former luxurious vegetation.

The eroded-out-weathered rhizoliths were further sub-classified into two types based on their field features: (i) those with brown-grey colors, hard and varnished (Figs. 3c; 5d); (ii) those with white-grey colors, fragile, and presenting fissures (Figs. 4b, c; 5e; 6b). The two subtypes of rhizoliths were formed and subjected to diagenesis in the same type of environment (mega-dunes) and share similar mineralogical characteristics based on SEM-EDS analyses. Nevertheless, the varnish observed on the first subtype of rhizoliths, hard in nature, indicates that they were formed earlier than the second, more fragile subtype. Indeed varnish formation takes a long time, with a stable geomorphic surface subjected to sunlight radiation (Watchman, 2000; Liu & Broecker, 2000, 2007; Xu et al., 2019). Of course, varnish might also depend on the type and mineralogy of the sediment and oxidation conditions. The laboratory results confirmed that all rhizoliths are constituted of calcium carbonate. Therefore, the first subtype of rhizoliths were eroded and weathered for a longer time than the second one, consistent with geomorphological processes, i.e. the fact that hard, varnished rhizoliths occurred predominantly in Order III belts.

These different features suggest that the rhizoliths were first formed at shallow

soil depth and later eroded out, with concomitant or subsequent modification of the root structure. The double layer walls (Fig. 5d) and the relicts (Figs. 5c,e) of the former roots further suggest that rhizoliths were likely formed around *Artemisia spp*. based on comparison with the characteristics of modern desert *Artemisia* spp. roots (cf. section 6.3).

6.2. Rhizolith distribution pattern

In the inner parts (Site A, B, C, Fig. 1) of the desert, rhizolith outcrops occur only in the windward gentle slopes of mega-dunes (Figs. 3a; 4a; 5a), on Orders II and III belts as the main outcrop areas. On Order I belts, rhizoliths were not found in the leeward slopes of the mega-dunes, which are steep and subjected to higher sedimentation rates than the windward slopes, with vegetation being quickly buried. Therefore, slipping sands in the leeward slopes do not provide a stable soil environment for vegetation and thus rhizolith formation.

In the southeastern margin of the desert (Fig. 1), rhizolith outcrops also occur, but only in the low dune areas and in the windward slopes of the swales where erosion takes place (Fig. 6a). No vegetation and rhizoliths were also observed in the leeward slopes.

Therefore, wind deflation and landforms are key parameters influencing the formation of rhizolith outcrops in the desert. The outcrops occur only in the windward slopes of dunes or in the swale beds and depressions, where deflation and erosion are transporting surface soil away, resulting in the exposure of the buried rhizoliths at the surface.

6.3. Vegetation

Rhizolith outcrops generally occur in the same area as living/dead *Artemisia* bushes rather than any other plants, or alternatively in bare zones without any plants.

The morphologies of the rhizoliths and their texture as well as their surface and inner structures (Figs. 4b, c; 5b, c, e) are identical or similar to those of modern living *Artemisia* roots, which are woody roots with cortex, stele, xylem but without a central hollow. Other kinds of vegetation such as *Psammochloa* and *Phragmites* also grow at or near the sampling sites, but the latter have herbaceous roots with a central hollow, in contrast with the collected rhizoliths.

The present results suggest that the decomposition of the dead *Artemisia* roots have triggered the rhizolith formation, where carbonate crystallization took place. *Artemisia* root decay or rhizosphere fungi may have provided oxalic acid and calcium oxalate crystals, with the microbial transformation of oxalate into carbonates leading to an increase in soil pH (Verrecchia et al., 2006; Dupraz et al., 2009; Huang et al., 2015). Alternatively, *Artemisia* dead roots might have provided a stable channel for continuously evaporation from the subsoil and so, calcification along the roots.

6.4. Soil and related environmental conditions

The field investigation suggested that soil moisture and the high porosity of sand provided the water and air required to sustain plant live and rhizolith formation, with in turn redox conditions favoring slow root decomposition and yielding enough CO_2 gas for HCO_3^- production.

Plants are growing in the dunes, which should not be considered as classical soils, but rather as aeolian sediments as defined in sedimentology and petrology. During their formation, the desert sediments are strongly affected by deflation due to their light texture and low density. The high dust accumulation rates do not let enough time for complete soil development (Sycheva, 2006). Consequently, quick denudation, erosion and deposition in the mega-dunes of the Badain Jaran desert prevent soil formation in this area.

The surface soils of the desert are aeolian loose sands with high porosity. Normally, below ca. 20-40 cm depth, the soils are wet (water content ~10%) (Wen et al., 2014; Wang et al., 2015a; Liu et al., 2016). Unfortunately, no systematic soil moisture measurement was performed in the desert, as it is too vast. Nevertheless, previous studies (Wen et al., 2014; Wang et al., 2015b; Liu et al., 2016) confirmed that the soil moisture in some swales and depressions is sufficient to allow *Artemisia* growth and rhizolith formation in windward slopes. It should be noted that soil moisture of the lower swales and depressions was likely higher than in the higher dunes based on vegetation distribution. The origin of soil and lake water remains controversial, whether from precipitation, condensation of atmospheric water, or groundwater (Ma & Edmunds., 2006; Wen et al., 2014; Jiao et al, 2015; Zhang et al., 2017; Yue et al., 2019).

Vegetation often grows in small patches or bands which are defined by the dune landforms. The regional landscape is characterized by mobile dunes and interdune lowlands. Stable and semi-stable eolian sandy soils are the dominant form. Previous results suggested that the effect of soil factors on vegetation characteristics was relatively weak and it is not possible to determine whether climate (e.g., the precipitation or temperature during the growing season) or geomorphology (e.g., parent materials) controls the vegetation communities in the desert (Wang et al., 2015b).

6.5. Climate

Modern climate of the desert is characterized by very low precipitation and high evaporation with strong northwestern wind. Comparatively, the sub-landscapes (mega-dunes), soil and vegetation on the vast desert are similar and even; but, the rhizolith outcrops are not evenly distributed everywhere in the desert. This shows that

local factors play a crucial role in rhizolith formation under arid climate. Rhizoliths are formed in loess sequences, under a more humid climate (e.g. Gocke et al., 2010) than in deserts, but also in the waterlogged soils of lake environments (Sun et al., 2019a). That implies that rhizoliths do not need specific aboveground climatic conditions. In the Badain Jaran Desert, the arid climate and intensive evaporation may favor carbonate precipitation and crystallization around dead roots in the highly porous sandy soils. This would explain the vast amount of rhizolith outcrops observed in the desert dunes.

6.6. Diagenesis and pedogenesis of rhizoliths in the sand-sedimentary environment

The above mentioned field features of rhizoliths from the Badain Jaran desert suggest that they were formed through diagenesis and pedogenesis in loose windblown sand sediments, at shallow depth and with open redox environmental conditions. The root relicts or hollows within the rhizoliths (Figs. 4c; 5b, c, e; 6d) indicate that the deceased roots served as an organic nucleus for carbonate precipitation within the rhizosphere, leading to the preservation of the root structure.

Based on the theory proposed by Dupraz et al. (2009), it can postulated that the organic carbon of the deceased roots was oxidized under optimal oxygen and soil moisture (i.e. weak redox) conditions at suitable depths, leading to the production of CO_2 used for $CaCO_3$ formation. Free Ca^{2+} ions could be derived from authigenic carbonates after *in situ* chemical weathering of soil primary silicate minerals such as feldspar, mica, amphibole and pyroxene (Dupraz, et al., 2005; Liu et al., 2011; Jin et al., 2015) due to low pH caused by organic matter decomposition and force-of-crystallization (Durand et al., 2010; Monger, 2014) and from the dissolution of *in situ* primary lithogenic carbonate rocks debris such as limestone and dolomite

(Sun et al., 2019b). The presence of free Ca^{2+} and local alkaline conditions through seasonal upwelling of alkaline water followed by evaporation (Arp et al., 2003) could lead to the nucleation of calcium carbonate on the root organic matrix (Arp et al., 1999a, b). The initiation of this process depends on the initial chemical composition of the root organic matter, as some organic functional groups have a high metal binding potential, inhibiting calcium carbonate mineral formation, whereas some others are more prompt to biotic and abiotic degradation, favoring calcium carbonate precipitation (Dupraz and Visscher, 2005).

Previous studies in the desert suggested that rhizoliths could be used as an indicator of precipitation intensity (Gao et al., 1993; Yang, 2000; Yang et al., 2003; Chen et al., 2004; Li et al., 2015a, b; Li et al., 2017; Zhu et al., 2019). Therefore, this work combined with previous research (Sun et al., 2019b) confirmed that such application is still uncertain. Rhizolith formation is strongly dependent on local conditions. Rhizolith formation is not a single function of climate but rather multiple environmental factors, e.g., geomorphology of dunefields, vegetation type, strength of pedogenesis, and existence of diagenesis. They could only be used as a local proxy of soil moisture and vegetation coverage, but cannot be applied to reconstruct past environmental conditions in such vast areas.

7. Conclusions and outlook

The formation mechanisms of rhizolith in desert remain poorly investigated, despite the large abundance of these objects in such settings and their importance for paleoenvironmental reconstructions. This study combined field and laboratory observations to better characterize the different types of rhizoliths in the Badain Jaran desert and constrain their formation conditions. Primary rhizoliths were shown to be

formed underground in soil of Badain Jaran desert before being brought out at the surface of the dunes where they are deflated and weathered due to the loose nature of the sandy soil and strong winds. Most of the rhizoliths presented a tube shape and occurred only in some parts of the desert, along the windward gentle slopes of mega-dunes. In contrast, the environmental conditions along the leeward steep slopes of the mega-dunes do not favor rhizoliths formation. Rhizoliths were formed only around dead roots of *Artemisia*. Rhizoliths and *Artemisia* bushes were indeed found to systematically co-exist in the swales and depressions between sub-dunes. Soil moisture plays an important role in *Artemisia* growth as well as rhizolith formation, taking into account the high porosity of sand soil and aridness of the climate. The results of the present study suggest that rhizoliths can only be used as a proxy for local soil moisture and vegetation cover, but are not able to indicate climate conditions directly above ground in a vast area, although the desert climate and the windward gentle slopes of mega-dunes are homogeneous or similar.

Further work is required to better understand the formation mechanism of the rhizoliths in deserts, taking into account the interrelations between vegetation type, environmental and climatic parameters.

Acknowledgements

We express special gratitude to the anonymous reviewers and the Editor-in-Chief, Professor Karl Stahr for their constructive and valuable comments to improve the paper. We would like to thank Wenhui Xue and Wentao Pei for their assistance during field exploration; Pu Wang for lab work; Professor Lijun Ling for photographing; Professor Hong Wang and Doctor Hanan Badawy for their detail revisions; Professor Viktor Golubtsov, and Doctor Eron Raines for their comments. Funding for this work

was provided by National Natural Science Foundation of China [No. 41561046 and M-0069 (Sino-German Mobility)].

References

Alonso-Zarza, A.M., Genise, J.F., Cabrera, M.C., Mangas, J., Martín-Pérez, A., Valdeolmillos, A., Dorado-Valiño, M., 2008. Mega-rhizoliths in Pleistocene aeolian deposits on Gran Canaria (Spain): ichnological and palaeoenvironmental significance. Palaeogeogr. Palaeoclimatol. Palaeoecol. 265, 39-61.

Arp, G., Reimer, A., Reitner, J., 1999a. Calcification in cyanobacterial biofilms of alkaline salt lakes. European J. Phycol. 34, 393-403.

Arp, G., Thiel, V., Reimer, A., Michaelis, W., Reitner, J., 1999b. Biofilm exopolymers control microbialite formation at thermal springs discharging into the alkaline Pyramid Lake, Nevada, USA. Sediment. Geol. 126, 159-176.

Arp, G., Reimer, A., Reitner, J., 2003. Microbialite formation in seawater of increased alkalinity, Satonda Crater Lake, Indonesia. J. Sediment. Res. 73, 105-127.

Bai, Y., 2011. Internal Structure and Formation Process of Mega-Dunes in the Badain Jaran Desert (in Chinese with English abstract). Doctoral dissertation. Lanzhou University.

Barta, G., 2011. Secondary carbonates in loess-paleosoil sequences: A general review. Centr. European J. Geosci. 3(2), 129-146.

Bojanowski, M.J., Jaroszewicz, E., Kosir, A., Lozinski, M., Marynowski, L., Wysocka, A., Derkiwski, A., 2016. Root-related rhodochrosite and concretionary siderite formation in oxygen-deficient conditions induced by a ground-water table rise. Sedimentol. 63 (3), 523–551.

Chen, J.S., Li, L., Wang, J.Y., Barry, D.A., Sheng, X.F., Gu, W.Z., Zhao, X., Chen, L.,

2004. Groundwater maintains dune landscape. Nature 432 (7016), 459-460.

Cramer, M.D., Hawkins, H. J., 2009. A physiological mechanism for the formation of root casts. Palaeogeogr. Palaeoclimatol. Palaeoecol. 274(3-4), 125-133.

Dickson, J. D. D., 1965. A modified staining technique for carbonate in thin section. Nature 205, 587

Dickson, J.D.D., 1966. Carbonate identification and diagenesis as revealed by staining. J. Sediment. Petrol. 61, 626-505.

Dong, Z.B., Qian, G.Q., Luo, W.Y., Zhang, Z.C., Xiao, S.C., Zhao, A.G., 2009. Geomorphological hierarchies for complex mega-dunes and their implications for mega-dune evolution in the Badain Jaran Desert. Geomorphol. 106, 180-185.

Dong, Z.B., Wang, T., Wang, X.M., 2004. Geomorphology of the megadunes in the Badain Jaran Desert. Geomorphol. 60, 191-203.

Dupraz, C. , Reid, R. P. , Braissant, O. , Decho, A. W. , Norman, R. S. , & Visscher, P. T., 2009. Processes of carbonate precipitation in modern microbial mats. Earth Sci. Rev. 96(3), 141-162.

Dupraz, C., Visscher, P.T., 2005. Microbial lithification in marine stromatolites and hypersaline mats. Trends Microbiol. 13, 429-438.

Durand, N., Monger, H.C., Canti, M.G., 2010. 9-Calcium carbonate features. In: Stoops, G., Marcelino, V., Mees, F. (Eds.), Interpretation of Micromorphological Features of Soils & Regoliths. Elsevier, pp. 149-194.

Gao, S., Chen, W., Jin, H., Dong, G., Li, B., Yang, G., Liu, L., Guan, Y., Sun, Z., Jin, J.,1993. Preliminary study on the Holocene desert evolution in the NW boundary of the Asia monsoon (in Chinese with English abstract). Ch. Sci. Ser. D 23, 202-208.

Gates, J., Edmunds, M., Darling, G., Ma, J., Pang, Z., Young, A., 2008. Conceptual

model of recharge to southeastern Badain Jaran Desert groundwater and lakes from environmental tracers. Appl. Geochem. 23, 3519-3534.

Gocke, M., Kuzyakov, Y., Wiesenberg, G.L.B., 2010. Rhizoliths in loess – evidence for postsedimentary incorporation of root-derived organic matter in terrestrial sediments as assessed from molecular proxies. Org. Geochem. 41, 1198-1206.

Gocke, M., Pustovoytov, K., Kühn, P., Wiesenberg, G.L.B., Löscher, M., Kuzyakov, Y., 2011. Carbonate rhizoliths in loess and their implications for paleoenvironmental reconstruction revealed by isotopic composition: $\delta^{13}C$, ^{14}C. Chem. Geol. 283, 251-260.

Gocke, M., Peth, S., Wiesenberg, G.L.B., 2014. Lateral and depth variation of loess organic matter overprint related to rhizoliths — revealed by lipidmolecular proxies and X-ray tomography. Catena 112, 72-85.

Golubtsov, V. A., Khokhlova, O. S., & Cherkashina, A. A., 2019. Carbonate Rhizoliths in Dune Sands of the Belaya River Valley (Upper Angara Region). Eurasian Soil Sci. 52(1), 83-93.

Gu, W.Z., Chen, J.S., Wang, J.Y., Zhao, X., Xie, M., Lu, J., Seiler, K. P., 2004. Challenge from the appearance of vadose water within the surface layer of megadunes, Badain Jaran dune desert, Inner Mongolia (in Chinese with English abstract). Adv. Water Sci. 15(6), 695–699

Hu, W., Wang, N., Zhao, L., Ning, K., Zhang, X., Sun, J., 2015. Surface energy and water vapor fluxes observed on a megadune in the Badain Jaran Desert, Ch. J. Arid Land 7, 579-589.

Huang, J., Huang, C., Liebman, M., 2015. J. Tradi. Ch. Med. 35(5), 594-599.

Huguet, A., Gocke, M., Derenne, S., Fosse, C., & Wiesenberg, G. L., 2013. Root-associated branched tetraether source microorganisms may reduce estimated

paleotemperatures in subsoil. Chem. Geol. 356, 1-10.

Huguet, A., Wiesenberg, G. L., Gocke, M., Fosse, C., & Derenne, S., 2012. Branched tetraether membrane lipids associated with rhizoliths in loess: Rhizomicrobial overprinting of initial biomarker record. Org. Geochem. 43, 12-19.

Jiao, J. J., Zhang, X., & Wang, X., 2015. Satellite-based estimates of groundwater depletion in the Badain Jaran Desert, Ch. Sci. Rep. 5(1), 8960

Jin, L., Edmunds, W. M., Lu, Z., & Ma, J., 2015. Geochemistry of sediment moisture in the Badain Jaran desert: Implications of recent environmental changes and water-rock interaction. Appl. Geochem. 63, 235-247.

Klappa, C.F., 1980. Rhizoliths in terrestrial carbonates: classification, recognition, genesis and significance. Sedimentol. 26, 613-629.

Kottek, M., J. Grieser, C. Beck, B. Rudolf, and F. Rubel, 2006: World Map of the Köppen-Geiger climate classification updated. Meteorol. Z. 15, 259-263. DOI: 10.1127/0941-2948/2006/0130.

Košir, A., 2004. *Microcodium* revisited: root calcification products of terrestrial plants on carbonate-rich substrates. J. Sediment. Res. 74 (6), 845-857.

Kraus, M.J. and Hasiotis, S.T., 2006. Significance of different modes of rhizolith preservation to interpreting paleoenvironmental and paleohydrological setting: Examples from paleogene paleosols, Bighorn Basin, Wyoming, U.S.A. J. Sediment. Res. 76, 633-646.

Li, Z., Wang, N., Cheng, H., Ning, K., Zhao, L., Li, R., 2015a. Formation and environmental significance of late Quaternary calcareous root tubes in the deserts of the Alashan Plateau, northwest China. Quat. Int. 372, 167-174.

Li, Z., Wang, N., Li, R., Ning, K., Cheng, H., & Zhao, L. 2015b. Indication of millennial-scale moisture changes by the temporal distribution of Holocene

calcareous root tubes in the deserts of the Alashan Plateau, Northwest China. Palaeogeogr. Palaeoclimatol. Palaeoecol. 440, 496-505.

Li, Z., Gao, Y., & Han, L., 2017. Holocene vegetation signals in the Alashan Desert of northwest China revealed by lipid molecular proxies from calcareous root tubes. Quat. Res. 88(1), 60-70.

Liu, T., & Broecker, W.S., 2000. How fast does rock varnish grow? Geol. 28 (2), 183-186.

Liu, T., & Broecker, W.S., 2007. Holocene rock varnish microstratigraphy and its chronometric application in the drylands of western USA. Geomorpho. 84, 1-21.

Liu, Z.H., Dreybrodt, W., Liu, H., 2011. Atmospheric CO_2 sink: silicate weathering or carbonate weathering? Appl. Geochem. 26, 292-294.

Liu, S., Lai, Z., Wang, Y., Fan, X., Wang, L., Tian, M., Jang, Y., & Zhao, H., 2016. Growing pattern of mega-dunes in the Badain Jaran Desert in China revealed by luminescence ages. Quat. Int. 410, 111-118.

Loope, D. B., 1988. Rhizoliths in ancient eolianites. Sed. Geol. 56, 301-314.

Ma, J., & Edmunds, W. M., 2006. Groundwater and lake evolution in the Badain Jaran Desert ecosystem, Inner Mongolia. Hydrogeol. J. 14, 1231-1243.

Monger, H. C., 2014. Soils as generators and sinks of inorganic carbon in geologic time. In: A.E. Hartemink and K. McSweeney (eds.), Soil Carbon. Prog. Soil Sci., 27-36.

Nascimento, D. L., Batezelli, A., & Ladeira, F. S., 2019. The paleoecological and paleoenvironmental importance of root traces: Plant distribution and topographic significance of root patterns in Upper Cretaceous paleosols. Catena 172, 789-806.

Owen, R.A., Owen, R. B., Renaut, R. W., Scott, J. J., Jones, B., Ashley, G. M., 2008. Mineralogy and origin of rhizoliths on the margins of saline, alkaline Lake

Bogoria, Kenya Rift Valley. Sed. Geol. 203, 143-163.

Pfefferkorn, H.W., Fuchs, K., 1991. A field classification of fossil plant substrate interactions. In: Neues Jahrbuch für G 648 eologie und Paläontologie, Abhandlungen 183, 17-36.

Rao, V. P. and Thamban, M., 1997. Dune associated calcrete, rhizoliths and paleosols from the Western Continental Shelf of India. J. Geo. Soc. In. 49, 297-306.

Rinehart, L.F., Lucas, S.G., Tanner, L., Nelson, W.J., Elrick, S.D., Chaney, D.S., DiMichele, W.A., 2015. Plant architecture and spatial structure of an early Permian woodland buried by flood waters, Sangre de Cristo Formation, New Mexico. Palaeogeogr. Palaeoclimatol. Palaeoecol. 424, 91-110.

Roberts, D. L. , Bateman, M. D. , Murray-Wallace, C. V. , Carr, A. S. , & Holmes, P. J., 2008. Last interglacial fossil elephant trackways dated by OSL/AAR in coastal aeolianites, Still Bay, South Africa. Palaeogeogr. Palaeoclimatol. Palaeoecol. 257(3), 261-279.

Sarjeant, W.A.S., 1975. Plant trace fossils. In: Frey, R.W. (Ed.), The Study of Trace Fossils. A Synthesis of Principles, Problems, and Procedures in Ichnology. Springer-Verlag, New York, pp. 51-69.

Sun, Q., Xue, W., Zamanian, K., Colin, C., Duchampalphonse, S., & Pei, W. 2019a. Formation and paleoenvironment of rhizoliths of Shiyang River Basin, Tengeri Desert, NW China. Quat. Int. 502, 246-257.

Sun, Q.F., Wang, H., Zamanian, K., 2019b. Radiocarbon age discrepancies between the carbonate cement and the root relics of rhizoliths from the Badain Jaran and the Tengeri deserts, Northwest China. Catena 180, 263-270.

Sycheva S.A., 2006. Long-term pedolithogenic rhytms in the Holocene. Quat. Int. 152, 181-191.

551 Verrecchia EP, Braissant O, Cailleau G., 2006. The oxalate–carbonate pathway in soil
552 carbon storage: the role of fungi and oxalotrophic bacteria. In book: Fungi in
553 Biogeochemical Cycles. Editor: G.M.Gadd. Chapter: 12. Cambridge University
554 Press. Cambridge. DOI: 10.1017/CBO9780511550522.013
555 Wang, X., Zhao, H., Yang, H., & Wang, K. 2019. Optical dating reveals that the
556 height of Earth's tallest megadunes in the Badain Jaran Desert of NW China is
557 increasing. J. Asian Earth Sci. 185, 104025
558 Wang, F., Sun, D., Chen, F., Bloemendal, J., Guo, F., Li, Z., Zhang, Y., Li, B., &
559 Wang, X., 2015. Formation and evolution of the Badain Jaran Desert, North
560 China, as revealed by a drill core from the desert centre and by geological
561 survey. Palaeogeogr. Palaeoclimatol. Palaeoecol. 426, 139-158.
562 Wang, M., Dong, Z., Luo, W., Lu, J., & Li, J., 2015a. Spatial variability of vegetation
563 characteristics, soil properties and their relationships in and around China's
564 Badain Jaran Desert. Env. Earth Sci. 74(9), 6847-6858.
565 Wang, M., Dong, Z. ,Lu, J. ,Li, J., Luo, W., Cui, X., Zhang, Y., Liu, Z., Jiao, Y.,
566 Yang, L., 2015b. Vegetation characteristics and species diversity around the
567 Badain Jaran Desert (In Chinese with English abstract). J. Desert Res. 35,
568 1226-1233.
569 Wang N A, Ma N, Chen H B, et al. 2013. A preliminary study of precipitation
570 characteristics in the hinterland of Badain Jaran Desert. Adv. Water Sci. 24(2),
571 153-160.
572 Wang, P., Clemens, S., Beaufort, L., Braconnot, P., Ganssen, G., Jian, Z., Kershaw, P.,
573 Sarnthein, M., 2005. Evolution and variability of the Asian monsoon system:
574 state of the art and outstanding issues. Quat. Sci. Rev. 24, 595-629.
575 Wang, Y., Cao, J., Zhang, X., Shen, Z., Mei, F., 2004. Carbonate content and carbon

and oxygen isotopic composition of surface soil in the dust source regions of China (In Chinese with English abstract). Mar. Geol. Quat. Geol. 24, 113-117.

Wang, H., Ambrose, S.H., Fouke, B.W., 2004. Evidence of long-term seasonal climate forcing in rhizolith isotopes during the last glaciation. Geophy. Res. Lett. 31(13), 718-730.

Watchman, A., 2000. A review of the history of dating rock varnishes. Earth Sci. Rev. 49(1-4), 261-277.

Xu, X., Li, Y., Li, Y., Lu, A., Qiao, R., Liu, K., Ding, H., & Wang, C., 2019. Characteristics of desert varnish from nanometer to micrometer scale: A photo-oxidation model on its formation. Chem. Geol. 522, 55-70.

Wen, J., Su, Z., Zhang, T., Tian, H., Zeng, Y., Liu, R., Kang, Y., & Der Velde, R. V., 2014. New evidence for the links between the local water cycle and the underground wet sand layer of a mega-dune in the Badain Jaran Desert, Ch. J. Arid Land 6(4), 371-377.

Yang, X., Scuderi, L., Paillou, P., Liu, Z., Li, H., Ren, X., 2011. Quaternary environmental changes in the drylands of China – A critical review. Quat. Sci. Rev. 30, 3219-3233.

Yang, X., Liu, T., & Xiao, H., 2003. Evolution of megadunes and lakes in the Badain Jaran Desert, Inner Mongolia, China during the last 31,000 years. Quat. Int. 104(1), 99-112.

Yang, X., 2000. Landscape evolution and precipitation changes in the Badain Jaran Desert during the last 30,000 years. Ch. Sci. Bull. 45, 1042-1047.

Yue, D.P., Zhao, J.B., Ma, Y.D., Huang, X.G., Shao, T.J., Luo, X.Q., Ma, A.H., 2019. Relationship between landform development and lake water recharge in the Badain Jaran Desert, China. Water 11, 1999.

https://www.mdpi.com/2073-4441/11/10/1999

Zhang, K., Cai, D., Ao, Y., An, Z., & Guo, Z., 2017. Local circulation maintains the coexistence of lake-dune pattern in the Badain Jaran desert. Sci. Rep. 7, 40238.

Zhao, J., Shao, T., Hou, Y., 2011. Moisture content of sand layer and its origin in a mega-dune area in the Badain Jaran Desert (in Chinese with English abstract). J. Nat. Resour. 26,694–702

Zhu, R., Li, Z., Gao, Y., Chen, Q., & Yu, Q., 2019. Variations in chemical element compositions in different types of Holocene calcareous root tubes in the Tengger Desert, NW China, and their palaeoenvironmental significance. Boreas 48(3), 800-809.

Zhu, J., Wang, N., Chen, H., Dong, C., & Zhang, H., 2010. Study on the boundary and the area of Badain Jaran Desert based on the remote sensing imagery (in Chinese with English abstract). Prog. Geogr. 29, 1087-1094.

Figures and Captions

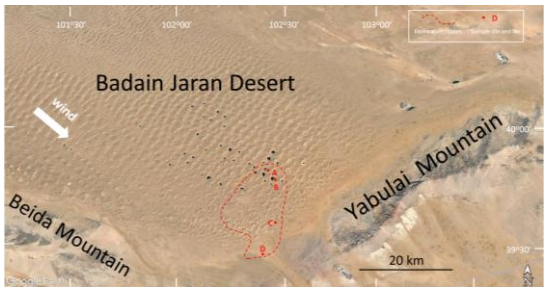

Fig. 1 Exploration route and sample sites in Badain Jaran Desert. Megadunes–ridges; Lakes—black dots; Exploration route—red dashed line; Sampling sites—A,B,C,D. A-Sumujilin Lake; B-Nuoertu Lake; C-Baoritaolegai Lakes; D-The Gate of National Geological Park of Badain Jaran Desert.

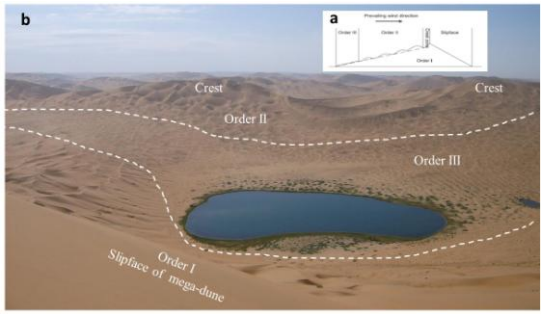

Fig.2 Conceptual typical (**a**, Dong et al., 2009) and field real (**b**) hierarchical orders in a compound megadune-lake system.

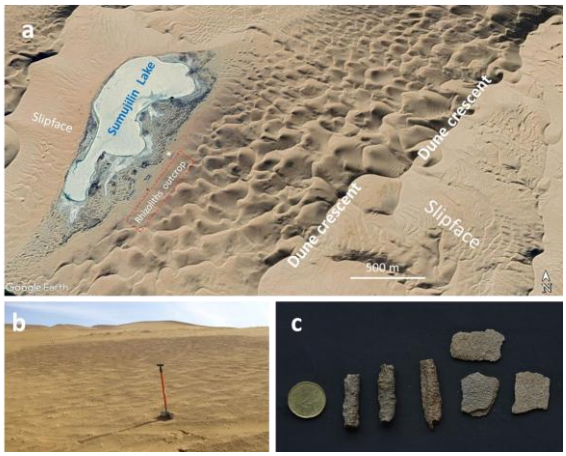

Fig. 3. Rhizoliths of Sumujinlin Lake. **a**-Rhizolith outcrops on the southeast side of the lake. **b**-Brown purple fragments of caliche and rhizoliths on the slope (the spade length is ~ 60 cm). **c**-Typical hard varnished rhizoliths and thick caliche fragments (the diameter of the coin is 20mm).

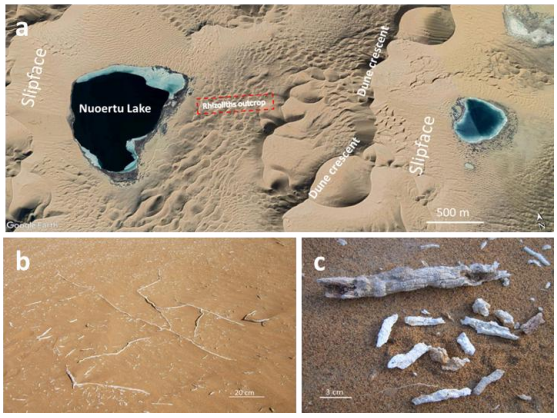

Fig. 4. Rhizoliths of Nuoertu Lake. **a**-Location of rhizolith outcrop, east side of Nuoertu Lake. **b**-White long branchy tubes of rhizoliths. **c**-Relicts of fine root hairs within a rhizolith tube.

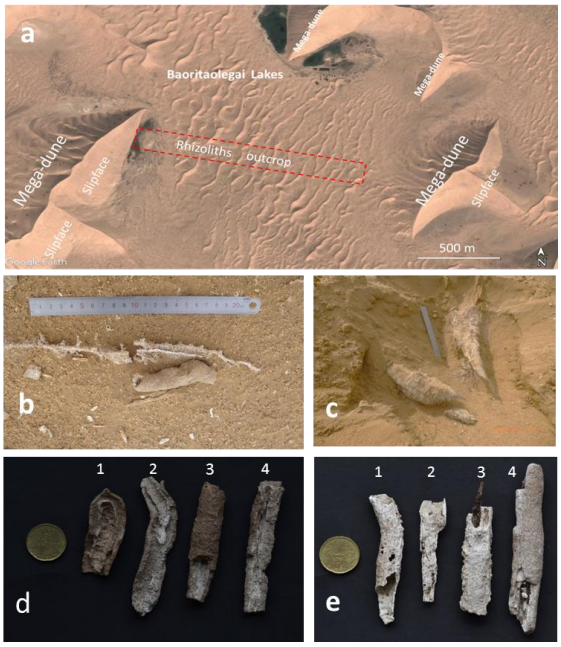

Fig.5. Rhizolith outcrops of Baoritaolegai Lakes. **a**-Location of rhizolith outcrops, south of Baoritaolegai lakes. **b**-Small and thin rhizolith tubes with lateral fine hair-like tubes and thick rhizolith tube with hemp rope-like striations. **c**-Loose sand particles are being cemented by carbonate around the deceased *Artemisia* roots within wet sand (the length of the ruler in the above photos is 20 cm). **d**-Double cemented layers (#1&2) and singular layer (#3&4) of the rhizolith walls. **e**-Plant relicts within rhizolith tubes and different thickness of tube walls. #1-2 have thin walls without plant relicts. #3-4 have thick walls containing plant relicts (the coin diameter in the above photos is 20 mm.).

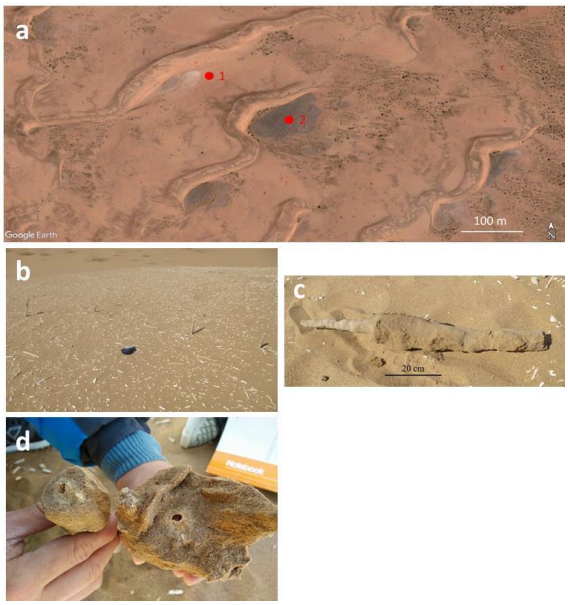

Fig. 6**.** Rhizoliths near to the Gate of National Geopark, Badain Jaran Desert. **a**-Rhizolith outcrops occur within the swales between the low dunes. #1 swale bed is white for enormous weathered fragments of rhizoliths and #2 swale bed is black due to pebbles from weathering of parent rocks underlying. The black dots are mainly *Artemisia* bushes. Singular barchan dune, barchan dune chains and erosional depressions can be observed at this site. **b**-Vertical rhizoliths and lying fragments of rhizoliths (the length of the camera bag is 12 cm). **c**-Primary rhizoliths dug out of soil in Fig **b**. **d**-Root relicts with central cavity and beige peripheral part of the primary rhizoliths.

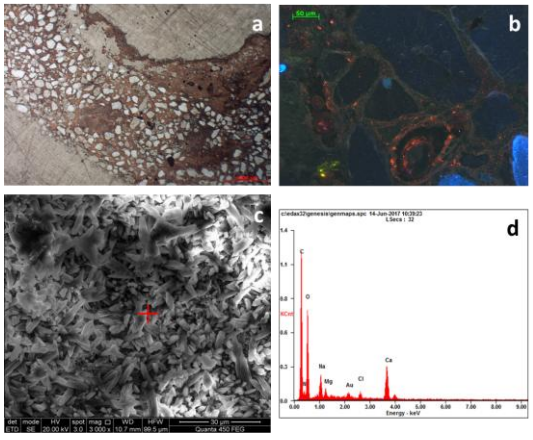

Fig.7. Micro-texture and composition of rhizoliths. **a**-Microscopy image of rhizolith cross-sections stained by Alizarin red S and potassium ferricyanide. The cement among particles was stained in dark purple red whereas the particles were not stained and remained bright in color (plane-polarized light, Baoritaolegai). **b**-Clastic particles and cement of rhizolith cross-section under cathodoluminescence. The light blue and green grains are feldspars; the deep dark grains are quartz. The small red orange dots are carbonates. Un-cathodoluminescene lighted cement may be clay minerals distributed in carbonate minerals, or may be caused by addition of Fe^{2+} and Mn^{2+} cations during the formation of the cement. In the bottom part of the picture, the dotted orange loop-like halos may be calcite derived from weathered feldspar grains (plane-polarized light, The Gate). **c**-SEM images of cement. **d**-EDS spectrum (of **c**) of the cement (The Gate).